C. R. Mecanique 347 (2019) 561–575

Contents lists available at ScienceDirect

Comptes Rendus Mecanique

www.sciencedirect.com

An empirical statistical constitutive relationship for rock joint shearing considering scale effect

Hang Lin [a,*], Shijie Xie [a], Rui Yong [b], Yifan Chen [a,*], Shigui Du [b]

[a] School of Resources and Safety Engineering, Central South University, Changsha, Hunan, 410083, China
[b] Ocean College, Zhejiang University, Zhoushan, Zhejiang 316000, China

ARTICLE INFO

Article history:
Received 29 April 2019
Accepted 5 August 2019
Available online 2 September 2019

Keywords:
Rock joints
Scale effect
Constitutive relationship
Statistical damage
Shear behavior

ABSTRACT

The scale effect of rock joint shearing is of great significance in rock engineering. Most existing shear constitutive models could describe the pre- and post-peak deformation of rock joints, but only in one particular scale, that is, those existing models will fail to depict the rock joint shearing in different length scales. Therefore, this study aims to establish a constitutive relationship for rock joints with considering the scale effect. Based on the assumption of a random statistical distribution of rock material strength and statistical mesoscopic damage theory, damage variables are defined as the ratio of the number of damaged elements to the total number in the shear process. Together with the nonlinear relationship between the microelement failure and the joint scale, an empirical statistical constitutive relationship for joint is established. And then, the determination method of constitutive relationship parameters and the variation laws with the scale are discussed. Results show that the predicted results of the proposed empirical relationship not only agree well with the experimental results but also fully describe nonlinear deformation, pre-peak softening, post-peak softening, residual stage, and other mechanical properties of the shear deformation of joint with different dimensions, thereby demonstrating the rationality of the constitutive relationship. The physical meaning of the constitutive relationship parameters is clear, and the expressions of the constitutive relationship parameters can be deduced from the experimental results. In addition, the influence of scale effect on the shear deformation of rock joints can be quantified using parameters, which help accurately describe the action form of scale effect.

1. Introduction

Rock joints significantly affect the mechanical properties of rock mass engineering and make rock mass significantly different from other media [1–6]. It has always been a hotspot in rock mechanics to establish a rock joints shear constitutive model which can accurately simulate the whole process of shear deformation and failure. Numerous scholars have conducted extensive and in-depth studies since the 1960s, thereby establishing numerous constitutive models of rock joints [7–10]. These representative models include the following: pure linear elastic constitutive models, such as Goodman's model [11]

* Corresponding authors.
E-mail addresses: linhangabc@126.com (H. Lin), xieshijieabc@126.com (S. Xie), yongrui_usx@hotmail.com (R. Yong), 1051361824@qq.com (Y. Chen), dushigui@126.com (S. Du).

https://doi.org/10.1016/j.crme.2019.08.001
1631-0721/

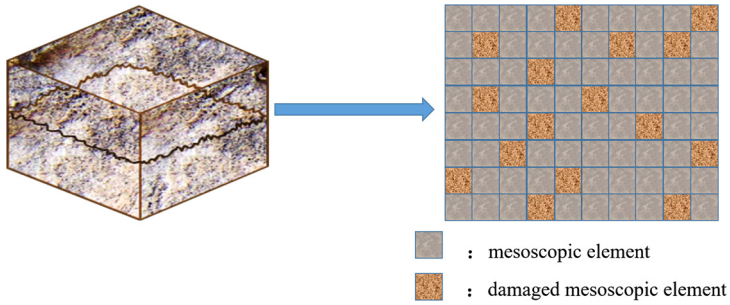

Fig. 1. Schematic diagram of damaged idealized rock joints.

and the Saeb–Amadei model [12]; nonlinear models, such as the Barton–Bandis model [13], the Grasselli model [14], and the CSDS model [15]; elastoplastic incremental models, including Plesha's model [16] based on the noncorrelated flow rule, Wang's model [17] reflecting anisotropy, and the DSC model [18] based on damage theory. The above-mentioned studies have deepened the deformation and strength of rock joints and have played an important role in the structural analysis and numerical simulation of rock mass engineering, including slope and tunnel [19–23]. However, given the complexity of rock joints, the existing constitutive models cannot fully describe the entire process deformation characteristics and damage evolution law of rock joints shear.

Meanwhile, some studies have also been conducted to investigate the effect of scale on the shear behavior of rock joints. Since Pratt, Black [24] first discovered the scale effect phenomenon in the direct shear test of natural rock joints, many researchers started to investigate this scale effect theoretically, experimentally and numerically. Barton and Choubey [25] emphasized that the scale effect of shear strength is closely related to that of JRC based on 136 sets of rock joint direct shear test results of eight rocks. Du, Huang [26] established the JRC scale effect fractal model based on the statistical law of roughness coefficient of 11064 rock joints surface contour curves. Ueng, Jou [27] conducted a direct shear test on standard model rock joints with a JRC of 18–20 and a size of 75–300 mm. The results indicated that a scale effect is closely related to surface morphology. Bahaaddini, Hagan [28] used PFC2D to study the relationship between rock joints shear behavior and scale. These findings contributed to the understanding of scale effect. However, given the complex mechanical behavior of rock materials, the mechanism and form of scale effect were partly elaborated, thereby suggesting a requirement for further investigations. Few shear constitutive models [29–32] consider the scale effect and post-peak damage softening property. Accurately and comprehensively reflecting the shear behavior of rock joints under various scales and establishing the shear constitutive model of rock joints that consider the scale effect has not been explored.

One of the classic explanations of scale effect is Weibull's statistical theory [33–36], which establishes the microstructural basis for the Weibull statistical parameters associated with the development of instability in a wing crack model. Tang, Yang [37], Tang, Liu [38] adopted the Weibull distribution to describe the microphysical properties of rocks and made good use of RFPA to reproduce the fracture process of rocks. These results indicate that the Weibull distribution is a good choice to describe the scale effect. Therefore, based on the theory of damage mechanics and Weibull distribution, a statistical constitutive empirical relationship of rock joint shear damage is proposed. The established empirical constitutive relationship is adopted to match the direct test results of different-scale rock joints. Finally, the effects of different scales on the damage evolution process of rock joints are further discussed.

2. Statistical constitutive relationship of rock joint damage considering the scale effect

2.1. Rock joint damage evolution relationship

Rock joints are substantially thinner than the rock wall on both sides. Thus, rock joints can be simplified into a thin layer with finite (small) thickness for the convenience of the present study. The thin layer can be regarded as the composition of numerous elements containing various rock material properties [39,40]. In the thin layer, damaged and undamaged mesoscopic elements are mixed, as shown in Fig. 1.

According to the damage mechanics, the damage of material is mainly an accumulation process of the mesoscopic elements [36,41–43]. Given the deterioration of the microstructure, the macroscopic physics will also present corresponding mechanical responses. The deformation and failure of rock joints are actually the formation, expansion, and penetration of microscopic defects in the thin layer. The definition of a damage variable is the basis of damage statistics theory applied to a rock joint damage constitutive model. Lemaitre [44] demonstrated that a classical damage model is established on the basis of the assumption of strain equivalence. It divides the rock–soil material S under load into the damaged and undamaged parts, and the effective stress $\tilde{\sigma}$ that acts on the undamaged part $\tilde{S}$ is equal to the nominal stress σ acting on the rock–soil material, that is,

$$\tilde{\sigma} = \sigma \frac{S}{\tilde{S}} = \frac{\sigma}{1 - D} \tag{1}$$

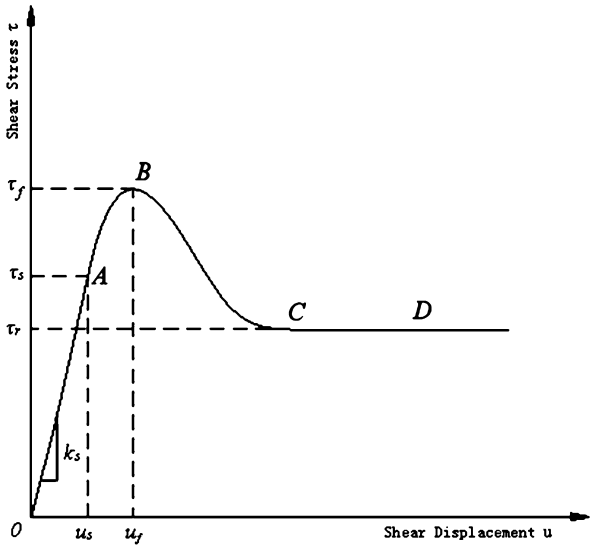

Fig. 2. Typical stress–shear displacement curve.

where D is the damage variable that takes a value between 0 and 1, corresponding to the damage states of the rock from undamaged to fully damaged.

However, the Lemaitre model considers the damaged part as non-load bearing. Thus, the total loss of bearing capacity when the rock–soil material is completely transformed into the damaged part, and its load-bearing capacity is 0. The Lemaitre model assumes that the damaged part cannot bear the load, which is evidently inconsistent with the residual strength properties of the rock material. In fact, the damaged material can also bear a certain load [45–48], that is, the nominal stress σ suffered by the rock and soil material is shared by two parts.

$$\sigma = \tilde{\sigma}(1 - D) + \sigma_{\mathrm{r}} D \tag{2}$$

where σ_{r} and D are the residual strength and damage variable, respectively.

The basic concept of the statistical damage constitutive model for rock joints is to establish a variable that links the complete state of the rock material to the damage state. This variable is known as damage variable D, which can be expressed as

$$D = \frac{N_{\mathrm{f}}}{N} \tag{3}$$

where N_{f} is the number of damaged mesoscopic elements under a certain loading, and N is the number of all mesoscopic elements.

The strength of the mesoscopic element follows the Weibull distribution function and its failure probability density function are

$$P(F_{\mathrm{a}}) = \begin{cases} 0 & F_{\mathrm{a}} < 0 \\ \frac{m}{F_0}\left(\frac{F_{\mathrm{a}}}{F_0}\right)^{m-1} \exp\left[-\left(\frac{F_{\mathrm{a}}}{F_0}\right)^{m}\right] & F_{\mathrm{a}} \geq 0 \end{cases} \tag{4}$$

where F_{a} is the shear strength of the mesoscopic element, F_0 and m are the distribution parameters.

Typical rock material damage models, such as the Mazars model [49] and the Sidoroff model, assume that the damage of rock material is zero or does not evolve before reaching the peak strength, and the damage only occurs after the peak stress. However, analyzing the shear stress–displacement curve of typical rock joints [50] indicates that the damage occurs not only after the peak. The typical joint shear process can be divided into the following phases [51] (Fig. 2): elastic phase (OA), pre-peak softening phase (AB), post-peak softening phase (BC), and residual phase (CD). Although the shear behavior of different tests is partly similar, the main features (yield shear stress τ_{s}; peak shear stress, τ_{f}; residual shear stress, τ_{r}; and shear stiffness, k_{s}) are the same.

In the OA section, the shear stress–displacement curve presents linear or nearly linear changes. That is, the microdefects in the material remain unchanged, without any damage occurring temporarily. In the section between the yield point and the peak value (AB section), the shear stress–displacement relationship has significantly deviated from the straight line, thus indicating that the damage to the rock material has occurred at this stage. The consideration of the yield point as the initial stage of damage is reasonable. For a mesoscopic element whose shear displacement is u, the threshold value for measuring whether it enters the damage state can be set as $F_{\mathrm{a}} = k_{\mathrm{s}} u - \tau_{\mathrm{s}}$ by referring to the Mohr–Coulomb criterion. The yield point

is the critical point between the elastic phase and the pre-peak softening phase, and the yield stress τ_s can be expressed as $\tau_s = k_s u_s$, similarly. In addition, the parameter F_0 can also be expressed as $F_0 = k_s u_0$. Thus, the failure probability density function (4) can be expressed as

$$P(u) = \begin{cases} 0 & u < u_s \\ \frac{m}{u_0}\left(\frac{u-u_s}{u_0}\right)^{m-1} \exp\left[-\left(\frac{u-u_s}{u_0}\right)^m\right] & u \geq u_s \end{cases} \tag{5}$$

In Eq. (5), the description of the damage process of the rock material has been transformed from studying the material's microscopic properties to characterizing its macroscopic properties. Damage occurs after the shear displacement reaches u_s. Then, the number of mesoscopic elements with damage (N_f) during the interval from u_s to u is

$$N_f = \int_{u_s}^{u} NP(u)\,du = N\left\{1 - \exp\left[-\left(\frac{u-u_s}{u_0}\right)^m\right]\right\} \tag{6}$$

The substitution of Eq. (6) into Eq. (3) yields

$$D = \begin{cases} 0 & u < u_s \\ 1 - \exp\left[-\left(\frac{u-u_s}{u_0}\right)^m\right] & u \geq u_s \end{cases} \tag{7}$$

Eq. (7) expresses the statistical damage evolution equation of rock joints shear deformation process.

2.2. Statistical constitutive relationship of rock joint damage

The total shear area of the mesoscopic element in the process of rock joint shear is denoted as S. The total cross-sectional area of the undamaged mesoscopic element is denoted as S_i, and the total cross-sectional area of the damaged mesoscopic element is signified as S_r. S can be expressed directly as

$$S = S_i + S_r \tag{8}$$

The force balance in the shear direction can be obtained as follows:

$$\tau S = \tau_i S_i + \tau_r S_r \tag{9}$$

Given the random distribution of damage in the rock material, the damaged material is mixed with the undamaged one, thereby making the size of the cross-sectional area of the damaged mesoscopic element S_r infeasible to determine accurately. As previously described, the material can be divided into damaged and undamaged parts once the damage occurs. Therefore, the ratio of the number of damaged mesoscopic elements N_f to the total number of mesoscopic elements N can be used to replace the ratio of the total cross-sectional area of the damaged mesoscopic element S_r to the total shear area of the mesoscopic element S to measure the damage variable D. The formulation of Eq. (3) is then modified as follows:

$$D = \frac{N_f}{N} = \frac{S_r}{S} \tag{10}$$

Referring to Eq. (2), Eq. (11) can be obtained by dividing both sides of Eq. (9) by S.

$$\tau = \tau_i(1 - D) + \tau_r D \tag{11}$$

The linear section load is all carried by the undamaged mesoscopic element. Thus, the effective shear stress $\tau_i = k_s u$. The substitution of $\tau_i = k_s u$ into Eq. (11) yields

$$\tau = k_s u(1 - D) + \tau_r D \tag{12}$$

When $D = 0$, the rock joints are positioned in an undamaged state. $\tau = k_s u$ corresponds to the linear phase of the shear stress–displacement curve. When $D = 1$, the rock joints are in a completely damaged state. In this case, $\tau = \tau_r$ corresponds to the residual phase of the shear stress–displacement curve. For Eq. (12) listed above, the units of k_s and u are MPa/mm and mm, respectively.

The substitution of Eq. (7) into Eq. (12) yields

$$\tau = \begin{cases} k_s u & u < u_s \\ (k_s u - \tau_r)\exp\left[-\left(\frac{u-u_s}{u_0}\right)^m\right] + \tau_r & u \geq u_s \end{cases} \tag{13}$$

Eq. (13) expresses the parameters u_0 and m. The key to establishing a reasonable shear damage constitutive relationship of rock joints is located in determining the specific expression of u_0 and m. The shear stress–displacement curve indicates that the slope is 0 at the peak, that is,

$$\frac{\mathrm{d}\tau}{\mathrm{d}u}\Big|_{u=u_\mathrm{f},\tau=\tau_\mathrm{f}}=0. \tag{14}$$

By combining the equation set of $\begin{cases} u=u_\mathrm{f} \\ \tau=\tau_\mathrm{f} \end{cases}$ with Eq. (14), the expressions of parameters u_0 and m can be obtained as follows:

$$\begin{cases} m=\dfrac{k_\mathrm{s}(u_\mathrm{f}-u_\mathrm{s})}{(k_\mathrm{s}u_\mathrm{f}-\tau_\mathrm{r})\ln\left(\frac{k_\mathrm{s}u_\mathrm{f}-\tau_\mathrm{r}}{\tau_\mathrm{f}-\tau_\mathrm{r}}\right)} \\ u_0=\dfrac{u_\mathrm{f}-u_\mathrm{s}}{\left[\ln\left(\frac{k_\mathrm{s}u_\mathrm{f}-\tau_\mathrm{r}}{\tau_\mathrm{f}-\tau_\mathrm{r}}\right)\right]^{\frac{1}{m}}} \end{cases} \tag{15}$$

By substituting Eq. (15) into Eq. (13), the shear damage constitutive relationship of rock joints without considering the scale effect can be obtained. It is worth mentioning here that Eq. (15) only applies to the case with obvious residual stress τ_r as shown in Fig. 2. If there is no constant residual stress in the test data, it is suggested to use the method of fitting data to get parameters m, u_0, and residual stress τ_r [29,52].

As previously mentioned, the damage is randomly distributed in the mesoscopic element, thereby resulting in the evident difference in the damage distribution on rock joints with various scales, which denote the variation in u_0 and m with scales. Sufficient experimental data [53] illustrate a close nonlinear relationship between parameters and scale when the Weibull distribution is adopted to describe the statistical constitutive relationship of rock material damage. In this case, a shear constitutive relationship of rock joints considering the scale effect can be established by further exploring such a nonlinear relationship between the two parameters and joint scale. Thus, the shear stress–displacement curve of joints in large scale can be predicted in accordance with that of joints in small scale. This outcome can provide a reference for constructing geotechnical engineering. Based on Eq. (7), the statistical constitutive relationship of shear damage of rock joints considering the scale effect is established as follows:

$$D=\begin{cases} 0 & u<u_\mathrm{s} \\ 1-\exp\left[-\left(\frac{u-u_\mathrm{s}}{u_0(s)}\right)^{m(s)}\right] & u\geq u_\mathrm{s} \end{cases} \tag{16}$$

where $u_0(s)$ and $m(s)$ are the nonlinear relationships between Weibull distribution parameters and rock joint scale, respectively.

Therefore, by substituting Eq. (16) into Eq. (13), the constitutive relationship for the shear behavior of rock joints considering scale effect can be obtained as follows:

$$\tau=\begin{cases} k_\mathrm{s}u & u<u_\mathrm{s} \\ (k_\mathrm{s}u-\tau_\mathrm{r})\exp\left[-\left(\frac{u-u_\mathrm{s}}{u_0(s)}\right)^{m(s)}\right]+\tau_\mathrm{r} & u\geq u_\mathrm{s} \end{cases} \tag{17}$$

In Eq. (17), the specific expression of the damage constitutive relationship can be obtained after specifically determining $u_0(s)$ and $m(s)$. The subsequent part verifies the rationality of the established constitutive relationship through relevant experimental data.

3. Constitutive relationship validation and discussion

3.1. Constitutive relationship validation

The rationality of the constitutive relationship is verified using the direct shear test data of series simulation rock joint in the work by Huang, Du [54]. In this experiment, the direct shear tests of simulation rock joint in scales of 20 cm × 20 cm–100 cm × 100 cm are taken under the normal stresses from 0.2 MPa to 1.0 MPa. The shear stress–displacement curves of the straight shear tests of J01 and J02 joints are obtained with many simulation rock joint tests, as presented in Figs. 3 and 4.

For data analysis, the method to obtain the required parameters of Eq. (13) from the test data is described as follows: The slope of the pre-peak region for data ranging between 25% and 90% of the peak shear stress is defined as the shear stiffness k_s [55]. The yield stress τ_s is defined as the stress corresponding to 90% of the peak shear stress τ_f, and the yield displacement u_s is derived from $\tau_\mathrm{s}=k_\mathrm{s}u_\mathrm{s}$ [56]. As for the residual stress τ_r, it can be found from Fig. 3 and Fig. 4 that when the direct shear experiment is completed, the curve still maintains a downward trend or fluctuates, and there is no obvious residual stress remaining constant as shown in Fig. 2. Of course, this phenomenon is very common in shear tests of natural joint replicas. However, this still causes some trouble for the value of τ_r in this paper, which affects the accuracy of solving m, u_0 by Eq. (15). Refer to the method of Liu and Yuan [29] and Tang, Xia [52], when the residual stress τ_r is not constant, the parameters m, u_0, and τ_r can be obtained by fitting to the experimental data. Therefore, this paper adopts the fitting method to get the parameters m and u_0 instead of Eq. (15).

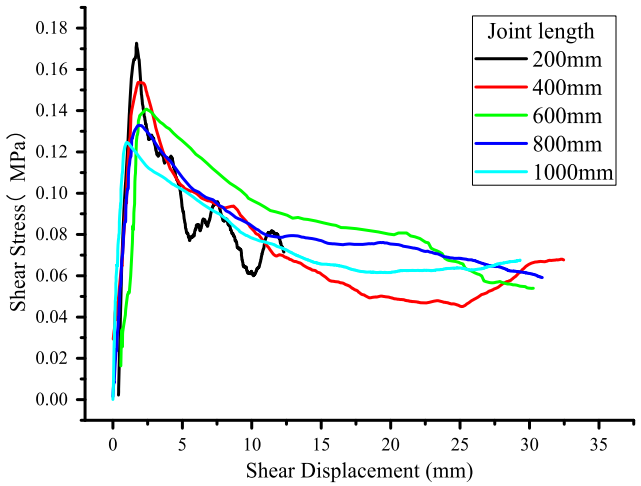

Fig. 3. Shear stress–displacement curves with J01 joint specimen.

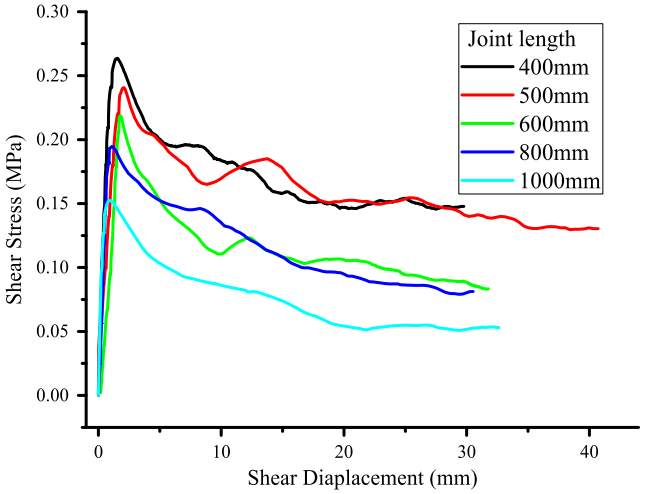

Fig. 4. Shear stress–displacement curves with J02 joint specimen.

The joint shear test data of J01-1000 mm and J02-1000 mm are taken as examples to verify the correctness of the constitutive relationship. According to the test results, the shear stiffness k_s corresponding to the J01 and J02 are 0.14095 and 0.2695, respectively. The yield displacement u_s corresponding to the J01 and J02 are 0.72451 and 0.4863, respectively. By substituting the corresponding k_s and u_s into Eq. (15), we have

$$\text{J01}: \tau = \begin{cases} 0.14095u & u < 0.7245 \\ (0.14095u - C)\exp\left[-\left(\frac{u-0.7245}{A}\right)^B\right] + C & u \geq 0.7245 \end{cases} \tag{18}$$

$$\text{J02}: \tau = \begin{cases} 0.2695u & u < 0.4863 \\ (0.2695u - C)\exp\left[-\left(\frac{u-0.4863}{A}\right)^B\right] + C & u \geq 0.4863 \end{cases} \tag{19}$$

where A, B, and C respectively refer to u_0, m, and τ_r.

The corresponding experimental data are substituted into Eqs. (18) and (19) to fit parameters A, B, and C and the results are shown in Figs. 5 and 6.

At this point, all parameters in the constitutive relationship expression are obtained, and the corresponding constitutive relationship equations can be obtained by substituting parameters A, B, and C into the constitutive relationship expression Eqs. (18) and (19):

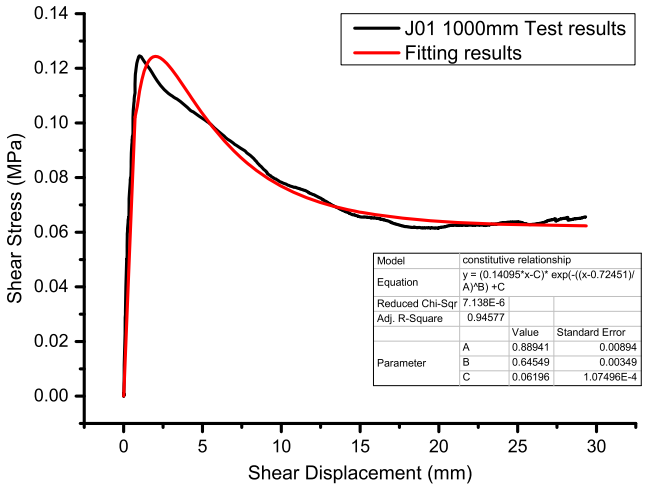

Fig. 5. Comparison between the theoretical curve of damage statistical constitutive relationship and J01 test result.

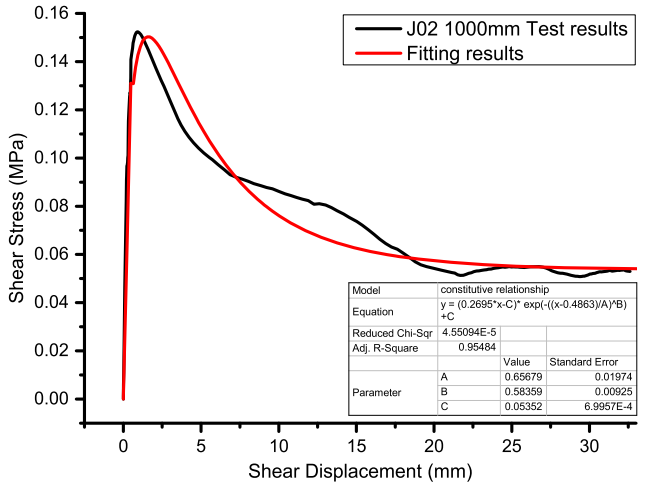

Fig. 6. Comparison between the theoretical curve of damage statistical constitutive relationship and J02 test result.

$$\text{J01}: \tau = \begin{cases} 0.14095u & u < 0.7245 \\ (0.14095u - 0.0619)\exp\left[-\left(\frac{u-0.7245}{0.8894}\right)^{0.6155}\right] + 0.0619 & u \geq 0.7245 \end{cases} \tag{20}$$

$$\text{J02}: \tau = \begin{cases} 0.2695u & u < 0.4863 \\ (0.2695u - 0.0535)\exp\left[-\left(\frac{u-0.4863}{0.6568}\right)^{0.5836}\right] + 0.0535 & u \geq 0.4863 \end{cases} \tag{21}$$

The fitting curves are plotted in Figs. 5 and 6, with the correlation coefficients of $R^2 = 0.945$ and $R^2 = 0.954$, thereby indicating that the established constitutive relationship in this study can accurately simulate the shear deformation process of rock joint.

Similarly, the fitting method is also used to obtain the parameters m and u_0 corresponding to the remaining experimental data in Figs. 3 and 4, and the processing process is the same as the example. The obtained parameter values and fitting correlation coefficients are presented in Tables 1 and 2, correspondingly. It should be noted that there is no regular relationship between the obtained residual stress, shear stiffness and size, so only the values of m and u_0 that have obvious relationship with size are listed in Tables 1 and 2. In Tables 1 and 2, the variation law between constitutive relationship parameters and joint size is illustrated in Figs. 7 and 8. In these figures, with the increase in the joint size, the values of both parameters generally show a power law decreasing trend. It is worth noting that the points in Fig. 7a seem to have a concave tendency, but this paper still uses a convex fitting relationship. According to some existing studies [53,57], when the Weibull distribution is used to describe the scale effect, the parameter $F_0(u_0)$ does show a convex trend with the increase of size.

Table 1
The constitutive relationship parameters corresponding to J01 specimen.

Joint length (m)	Parameter u_0	Parameter m	R^2
0.4	1.6598	0.7772	0.8512
0.6	1.4277	0.6610	0.8560
0.8	1.1842	0.6248	0.8616
1.0	0.8890	0.6150	0.9550

Table 2
The model parameters corresponding to J02 specimen.

Joint length (m)	Parameter u_0	Parameter m	R^2
0.4	1.5059	0.7165	0.9322
0.5	1.4128	0.7056	0.8177
0.6	1.2250	0.6680	0.9080
0.8	0.7310	0.6220	0.8623
1.0	0.6568	0.5836	0.9335

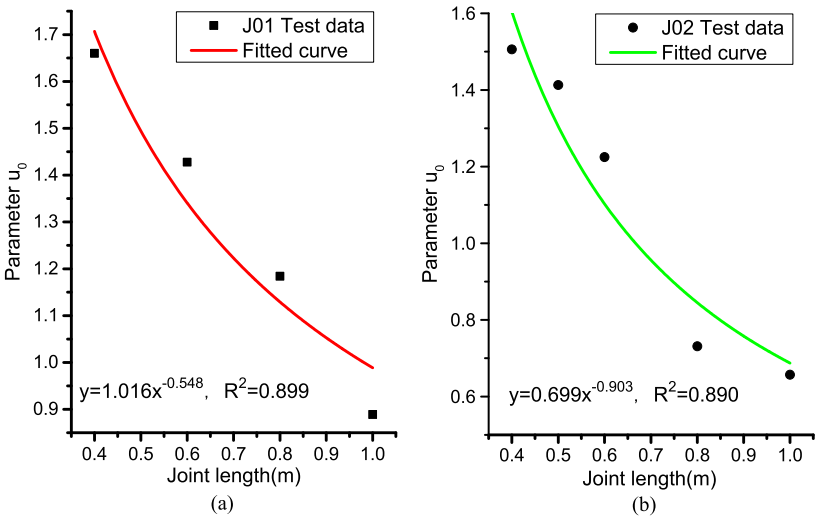

Fig. 7. Relationship between constitutive relationship parameter u_0 and joint length. (a) J01, (b) J02.

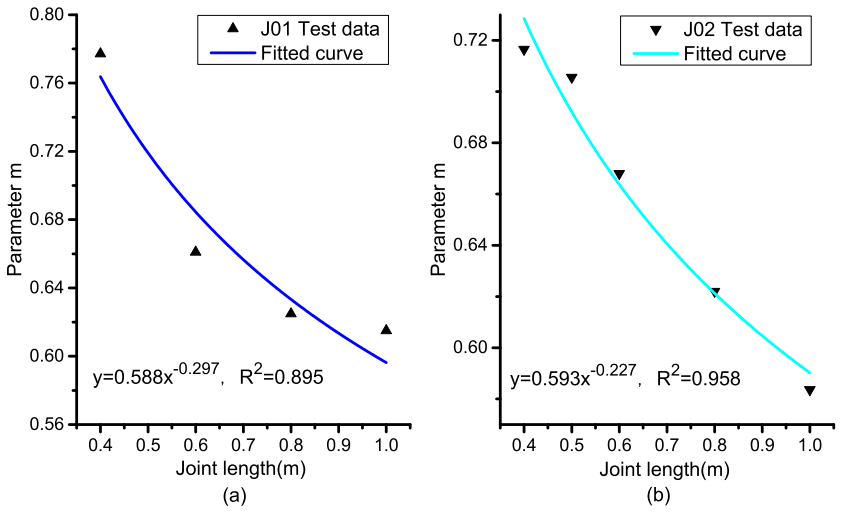

Fig. 8. Relationship between constitutive relationship parameter m and joint length. (a) J01, (b) J02.

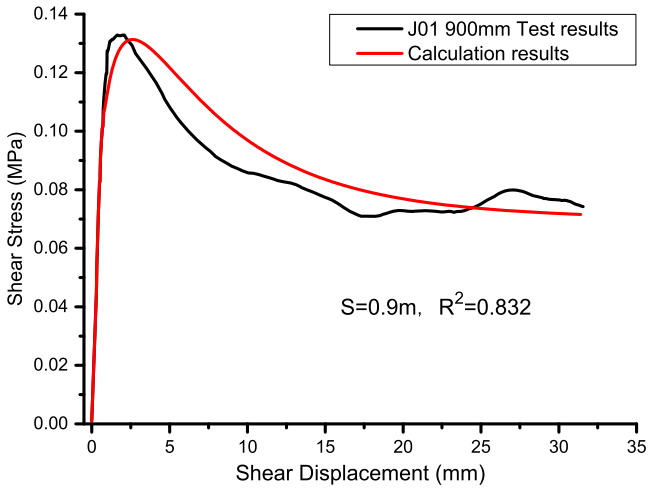

Fig. 9. Comparison of results from the theoretical curve of damage statistical constitutive relationship and test.

Table 3
Value of relevant parameters.

Parameter	Value
k_s	1.4336
u_s	1.5025
τ_r	1.51
m	0.98
u_0	0.85

The fitting relationship between the joint scale S of J01 and J02 and the parameters u_0 and m can be obtained from Figs. 7 and 8, as expressed in Eqs. (22) and (23), respectively.

$$\left.\begin{array}{ll} u_0 = 1.016S^{-0.548}, & R^2 = 0.853 \\ m = 0.588S^{-0.297}, & R^2 = 0.826 \end{array}\right\} \tag{22}$$

$$\left.\begin{array}{ll} u_0 = 0.699S^{-0.903}, & R^2 = 0.883 \\ m = 0.594S^{-0.227}, & R^2 = 0.919 \end{array}\right\} \tag{23}$$

The previous discussion of the relationship between parameters and joint scale reveals a power function relationship between parameters and joint size. This relationship can be expressed as $y = Ax^{-B}$, where A and B are constants that depend on rock joints types and can be determined on the basis of the fitting analysis of test data. By substituting the fitting equation into Eq. (17), the joint shear constitutive relationship considering the scale effect can be obtained. For example, $S = 0.9$ (J01-900 mm joint specimen) is substituted into Eq. (22) to obtain the corresponding parameter $u_0 = 1.07639$ and $m = 0.60669$. Fig. 9 presents the comparison between the theoretical curves obtained using the constitutive relationship established in this study and the test results of the specific scale joints (900 mm). The theoretical curve exhibited in Fig. 9 agrees well with the experimental results, thereby indicating the rationality and correctness of the established constitutive relationship.

3.2. Constitutive relationship discussion

As previously described, the parameters m and u_0 severally affect the geometric scale and shape of the shear stress–displacement curve, which is of great significance to the feasibility and capability of the constitutive relationship proposed. Section 3.1 demonstrates that the parameters of the damage statistical constitutive model show a power function decreasing trend with the increase in joint size. The influence of different joint sizes on the shear stress–displacement curve is reflected in the influence on constitutive relationship parameters. Therefore, the law of the shear stress–displacement curve changing with joint size can be analyzed through the single variable method to reflect the influence of constitutive relationship parameters on the shear stress–displacement curve. For Eq. (16), the single-variable method is adopted to change u_0 and m respectively to obtain the corresponding variation curves, and these relevant parameters used are given in Table 3.

The variation of the shear stress–displacement curve under different parameters u_0 are elaborated in Fig. 10. It can be concluded from Fig. 10 that the curve groups after the yield stage under the conditions different u_0 are approximately parallel. The peak shear stress decreases with the parameter u_0; that is, the peak shear stress decreases with the increase in joint scale. This phenomenon is consistent with the general cognition of the scale effect, thereby confirming the correctness

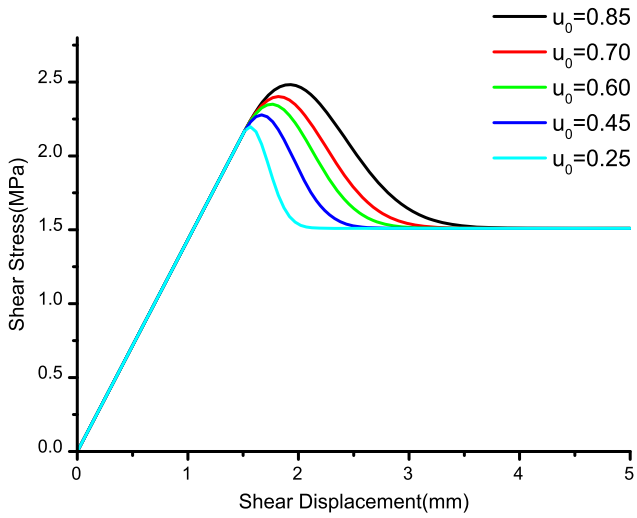

Fig. 10. Influence of parameter u_0 on the constitutive relation.

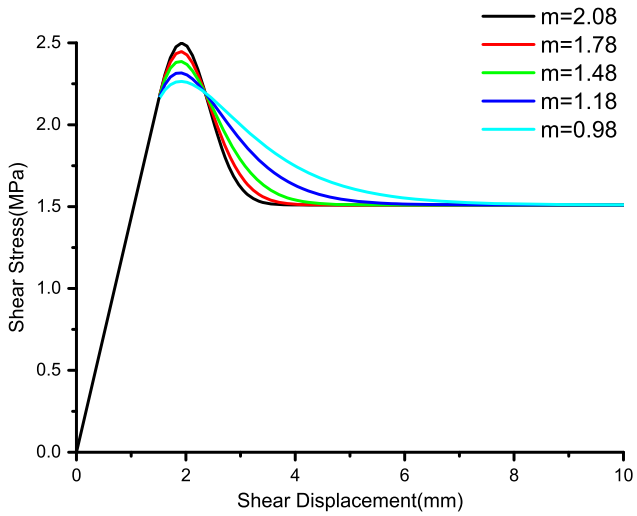

Fig. 11. Influence of parameter m on the constitutive relation.

of the constitutive relationship. A point with such characteristics is defined as the starting point of the residual phase of the shear process (point C in Fig. 2): the shear stress at this point subtracted the residual stress to get a difference value, the ratio of the difference value to the residual stress should be less than 10^{-6}. During the process of parameter u_0 increasing from 0.25 to 0.85, the peak shear stress increases by 15.43%, and the shear displacement required to reach the residual stage increases by 54.09%. Such an influence on the relationship of the shear constitutive relationship is mainly reflected in the damage development stage after the yield point. Thus, the parameter u_0 is the reflection of the macroscopic statistical average strength of rock materials.

The changes in shear stress–displacement curve for various parameter m are illustrated in Fig. 11. It can be clearly seen from Fig. 11 that with the increase of parameter m, the peak shear stress gradually increases and the post-peak part of the shear stress–displacement curve gradually becomes steep. When the parameter m changes from 0.98 to 2.08, the elastic phase of the shear stress–displacement curve remains unchanged, while the peak shear stress increases by 14.3%. By contrast, the shear displacement required for the curve to reach the residual phase increased by 168.49%. It is worth noting that residual stress, as an inherent property of rock materials, remains constant no matter how the parameters u_0 and m change. It is an interesting phenomenon in Fig. 11 that the stress–displacement curves corresponding to different m intersect at the same point, which is located between the peak stress and the residual stress. The variation trend of curves before and after the intersection point is opposite. The larger the parameter m is, the greater the absolute value of the slope of the shear stress–displacement curve at the pre-peak and post-peak stages (the steeper the curve is), indicating that m mainly reflects the concentration of the strength distribution of the internal unit of rock material.

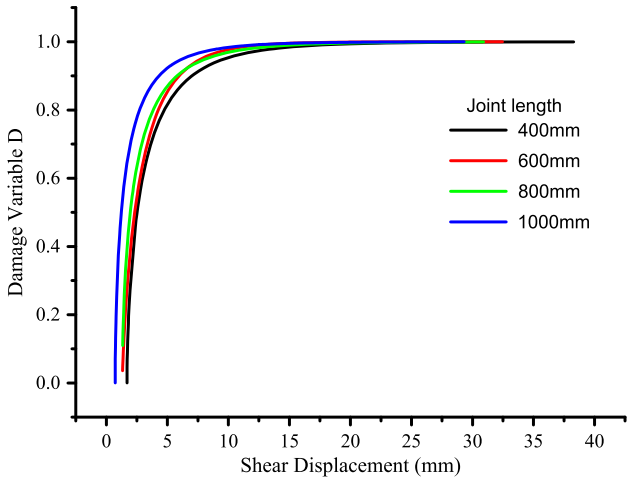

Fig. 12. Influence of joint size on the damage variable.

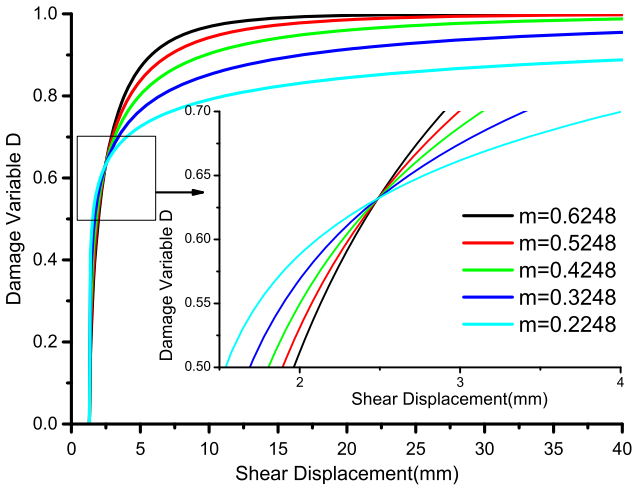

Fig. 13. Damage variable of joints with different parameters m.

Table 4
Parameters of damage variable.

Parameter	Value
u_s	1.3044
m	0.6248
u_0	1.1842

3.3. Damage evolution process

The data obtained from multiple shear tests [54] are substituted into Eq. (7) to draw typical damage evolution curves of joints with different lengths, as depicted in Fig. 12. In this figure, the damage performance of joints with different sizes is nearly the same: the damage change in the rock joints accelerates with the increase in joint size, and the shear displacement required from the beginning of damage ($D = 0$) to complete damage ($D = 1$) is reduced. In combination with Eq. (16) and the relationship between constitutive relationship parameters and size discussed above, the influence of joint size on damage characteristics can be reflected by the change in damage characteristics under various parameters.

The relationship between damage variable D and shear displacement under different parameters (various sizes) is demonstrated in Figs. 13 and 14, respectively, thereby showing examples of the variations in the damage variable, which is calculated using the damage evolution relationship, at different shear displacement for various joint scales (values of parameter). These relevant parameters used in Figs. 13 and 14 are shown in Table 4. In Figs. 13 and 14, joint length significantly influences the damage evolution process of rock joints. With the increase in joint length (the decrease in parameters m and u_0), the damage variables that correspond to the same shear displacement show a decreasing trend. With the increase

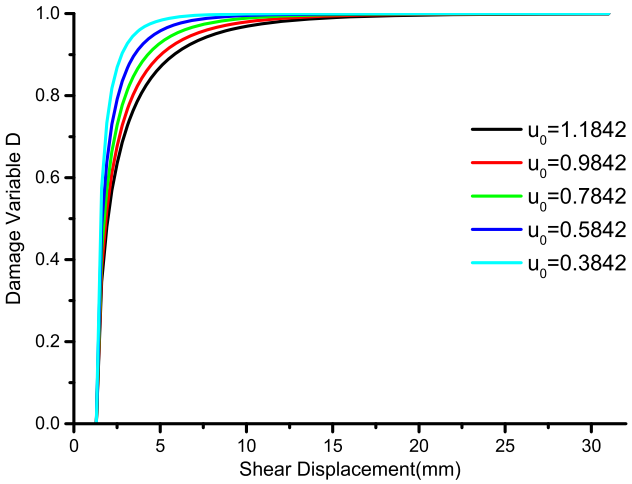

Fig. 14. Damage variable of joints with different parameters u_0.

Table 5
Results of direct shear tests [58].

σ_n (MPa)	u_s (mm)	u_f (mm)	τ_f (MPa)	τ_r (MPa)
50	0.9825	1.1755	46.3512	31.2801

in m, the shear displacement required to achieve complete damage ($D = 1$) is small, and the curvature of damage evolution curve increases. By contrast, with the increase in u_0, the shear displacement required to achieve complete damage is large, and the curvature of damage evolution curve is reduced. Therefore, the two parameters play opposite roles in the growth rate of damage variables. Parameters m and u_0 increase using the same amplitude, and the influence of m on the shear displacement and curvature required for the joint damage to reach the complete state is evident. The law of joint damage relation of different scales changing with parameters is of certain reference significance for finding precursor information of rock mass from stability to failure and implementing stability monitoring and disaster warning.

3.4. Discussion on model applicability

In section 3.1, the data fitting method was used to determine parameters m and u_0. In this section, the process of parameters solving m and u_0 by Eq. (15) was demonstrated through an example with constant residual stress, and the constitutive relationship expression was obtained to illustrate the correctness of the constitutive relationship established in this paper.

In order to investigate the regularities of the shear strength, shear deformation and other mechanical properties of joint rock mass with different roughness values under compression-shear stress, Zhou H, Cheng GT [58] prepared marble specimens with dentate heights of 0, 1 and 3 mm respectively. Then direct shear tests were conducted on the marble specimens under different normal stresses. As shown in Fig. 15, the test data with $h = 3$ mm and normal stress of 50 MPa was selected for our analysis. The test results are shown in Table 5. According to the test results, the shear stiffness k_s corresponding to the normal stress 50 MPa tests is 41.98. By substituting the relevant data in Table 4, u_s, u_f, τ_f, τ_r, and k_s into Eq. (15), we have:

$$\sigma_n = 50 \text{ MPa} \ : \ \begin{cases} m = & 2.4729 \\ u_0 = & 0.3849 \end{cases} \tag{24}$$

At this point, all parameters in the model expression are obtained, and the corresponding model equations can be obtained by substituting relevant test data into the model expression – Eq. (13) – at last:

$$\tau = \begin{cases} 41.98u & u < 0.9825 \\ (41.98u - 31.2801)\exp\left[-\left(\frac{u-0.9825}{0.3849}\right)^{2.4729}\right] + 31.2801 & u \geq 0.9825 \end{cases} \tag{25}$$

The shear behaviors obtained from experimental tests and those estimated by the proposed models are compared as shown in Fig. 16. The correlation coefficients ($R^2 = 0.979$) show excellent consistency between the constitutive relationship prediction and the experimental results.

In conclusion, the constitutive relationship established in this paper has wide applicability. For the shear stress–displacement curve with constant residual stress, it can be solved by Eq. (15) and relevant experimental data. For the

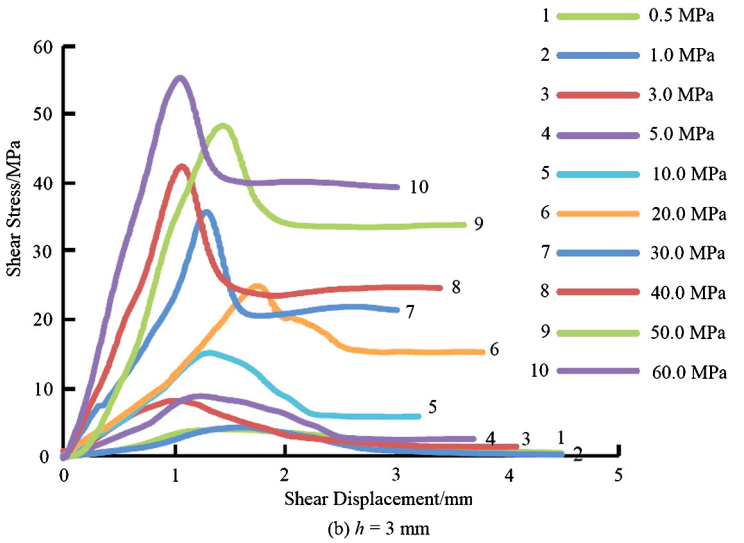

Fig. 15. Relation curves of shear stress and shear displacement under different normal stresses.

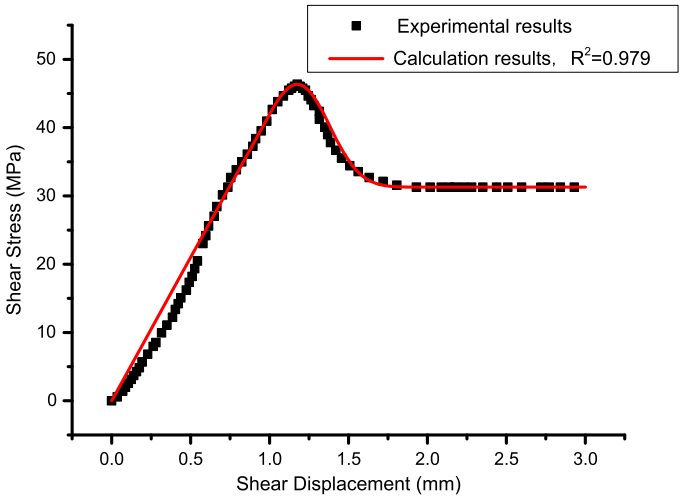

Fig. 16. Comparisons between the shear behaviors obtained in tests [58] and those estimated by the proposed constitutive relationship.

shear stress–displacement curve without constant residual stress, it can be solved by a fitting method, which also has good fitting accuracy.

4. Conclusion

(1) Based on the assumption of the random statistical distribution of the strength of rock material micro-elements, an empirical statistical constitutive relationship of joint shear damage with the scale effect is established by combining the damage mechanics and considering the nonlinear relationship between the damage evolution process and joint size.

(2) The curve of the constitutive relationship established in this study agrees well with the test curve. Thus, this constitutive relationship can reflect the whole process of shear deformation of rock joints, especially the characteristics of the post-peak residual stage. The constitutive relationship has few parameters with clear physical meaning, thus indicating its superiority.

(3) Based on the joint experimental results of different scales, the relationship between constitutive relationship parameters and size is discussed, and the empirical formula for the parameters of the constitutive relationship considering the scale effect is expressed. The parameters of the large-scale joints predicted by the formula are substituted into the constitutive relationship, and the predicted curves present significant consistency with the test results.

Acknowledgements

This paper gets its funding from project (51774322) supported by National Natural Science Foundation of China; Project (2018JJ2500) supported by Hunan Provincial Natural Science Foundation of China. The authors wish to acknowledge these supports.

References

[1] Y. Zhao, L. Zhang, W. Wang, J. Tang, H. Lin, W. Wan, Transient pulse test and morphological analysis of single rock fractures, Int. J. Rock Mech. Min. Sci. 91 (2017) 139–154.
[2] C. Zhang, C. Pu, R. Cao, T. Jiang, G. Huang, The stability and roof-support optimization of roadways passing through unfavorable geological bodies using advanced detection and monitoring methods, among others, in the Sanmenxia Bauxite Mine in China's Henan Province, Bull. Eng. Geol. Environ. (2019), https://doi.org/10.1007/s10064-018-01439-1.
[3] Y. Wang, H. Lin, Y. Zhao, X. Li, P. Guo, Y. Liu, Analysis of fracturing characteristics of unconfined rock plate under edge-on impact loading, Eur. J. Environ. Civ. Eng. (2019) 1–16, https://doi.org/10.1080/19648189.2018.1509021.
[4] Y. Zhang, N. Huang, Numerical study on the shear-flow behavior and transport process in rough rock fractures, C. R. Mecanique 346 (2018) 877–886, https://doi.org/10.1016/j.crme.2018.05.006.
[5] Y. Shen, Y. Wang, Y. Yang, Q. Sun, T. Luo, H. Zhang, Influence of surface roughness and hydrophilicity on bonding strength of concrete-rock interface, Constr. Build. Mater. 213 (2019) 156–166.
[6] H. Lin, Z. Xiong, T. Liu, R. Cao, P. Cao, Numerical simulations of the effect of bolt inclination on the shear strength of rock joints, Int. J. Rock Mech. Min. Sci. 66 (2014) 49–56, https://doi.org/10.1016/j.ijrmms.2013.12.010.
[7] J.Y. Shen, M. Karakus, Determination of Mohr–Coulomb shear strength parameters from generalized Hoek–Brown criterion for slope stability analysis, Rock Mech. Rock Eng. 45 (2012) 123–129.
[8] J. Shen, R. Jimenez, Predicting the shear strength parameters of sandstone using genetic programming, Bull. Eng. Geol. Environ. (2018) 1–16.
[9] F. Huang, J. Shen, M. Cai, C. Xu, An empirical UCS model for anisotropic blocky rock masses, Rock Mech. Rock Eng. (2019) 1–13.
[10] Y. Xu, F. Dai, T. Zhao, N.W. Xu, Y. Liu, Fracture toughness determination of cracked chevron notched Brazilian disc rock specimen via griffith energy criterion incorporating realistic fracture profiles, Rock Mech. Rock Eng. 49 (2016) 1–11.
[11] R.E. Goodman, R.L. Taylor, T.L. Brekke, Closure on a model for the mechanics of jointed rock, J. Soil Mech. Found. Div. 94 (1970) 637–660.
[12] S. Saeb, B. Amadei, Modelling rock joints under shear and normal loading, Int. J. Rock Mech. Min. Sci. Geomech. Abstr. (1992) 267–278.
[13] S. Bandis, A. Lumsden, N. Barton, Fundamentals of rock joint deformation, Int. J. Rock Mech. Min. Sci. Geomech. Abstr. 20 (1983) 249–268.
[14] G. Grasselli, Manuel rocha medal recipient shear strength of rock joints based on quantified surface description, Rock Mech. Rock Eng. 39 (2006) 295.
[15] R. Simon, M. Aubertin, H. Mitri, A non-linear constitutive model for rock joints to evaluate unstable slip. Vail Rocks 1999, in: Proc. 37th US Symposium on Rock Mechanics (USRMS), American Rock Mechanics Association, 1999.
[16] M.E. Plesha, Constitutive models for rock discontinuities with dilatancy and surface degradation, Int. J. Numer. Anal. Methods Geomech. 11 (2005) 345–362.
[17] J. Wang, Y. Ichikawa, C. Leung, A constitutive model for rock interfaces and joints, Int. J. Rock Mech. Min. Sci. 40 (2003) 41–53.
[18] C.S. Desai, Y. Ma, Modelling of joints and interfaces using the disturbed-state concept, Int. J. Numer. Anal. Methods Geomech. 16 (1992) 623–653.
[19] X.P. Zhou, J. Bi, Q.H. Qian, Numerical simulation of crack growth and coalescence in rock-like materials containing multiple pre-existing flaws, Rock Mech. Rock Eng. 48 (2015) 1097–1114.
[20] A. Liu, G. Tian, Q. Zhang, W. Lin, J. Jiang, Shear relaxation characteristics of rock joints under stepwise loadings, C. R. Mecanique 346 (2018) 1179–1191, https://doi.org/10.1016/j.crme.2018.09.001.
[21] R. Sahlaoui, K. Sab, J-V. Heck, Yield strength of masonry-like structures containing thin adhesive joints: 3D or 2D-interface model for the joints? C. R. Mecanique 339 (2011) 432–438, https://doi.org/10.1016/j.crme.2011.03.018.
[22] Y.F. Chen, H. Lin, Consistency analysis of Hoek–Brown and equivalent Mohr–Coulomb parameters in calculating slope safety factor, Bull. Eng. Geol. Environ. (2018) 1–13, https://doi.org/10.1007/s10064-018-1418-z.
[23] J. Shen, M. Karakus, Three-dimensional numerical analysis for rock slope stability using shear strength reduction method, Can. Geotech. J. 51 (2014) 164–172.
[24] H. Pratt, A. Black, W. Brown, W. Brace, The effect of speciment size on the mechanical properties of unjointed diorite, Int. J. Rock Mech. Min. Sci. Geomech. Abstr. (1972) 513–516.
[25] N. Barton, V. Choubey, The shear strength of rock joints in theory and practice, Rock Mech. Rock Eng. 10 (1977) 1–54.
[26] S. Du, M. Huang, Z.Y. Luo, R.D. Jia, Y.M. Wang, Scale effects of undulation amplitude of rock joints, Q. J. Eng. Geol. (2010).
[27] T-S. Ueng, Y-J. Jou, I-H. Peng, Scale effect on shear strength of computer-aided-manufactured joints, J. Geoengin. 5 (2010) 29–37.
[28] M. Bahaaddini, P. Hagan, R. Mitra, B. Hebblewhite, Scale effect on the shear behaviour of rock joints based on a numerical study, Eng. Geol. 181 (2014) 212–223.
[29] H. Liu, X. Yuan, A damage constitutive model for rock mass with persistent joints considering joint shear strength, Can. Geotech. J. 52 (2015) 3107–3117.
[30] J-J. Dong, Y-W. Pan, A hierarchical model of rough rock joints based on micromechanics, Int. J. Rock Mech. Min. Sci. Geomech. Abstr. (1996) 111–123.
[31] F. Vallier, Y. Mitani, M. Boulon, T. Esaki, F. Pellet, A shear model accounting scale effect in rock joints behavior, Rock Mech. Rock Eng. 43 (2010) 581–595, https://doi.org/10.1007/s00603-009-0074-9.
[32] Y. Wang, P. Guo, X. Li, H. Lin, Y. Liu, H. Yuan, Behavior of fiber-reinforced and lime-stabilized clayey soil in triaxial tests, Appl. Sci. 9 (2019) 900.
[33] W. Weibull, A statistical distribution function of wide applicability, J. Appl. Mech. 18 (1951) 293–297.
[34] J. Ji, C. Zhang, Y. Gao, J. Kodikara, Reliability-based design for geotechnical engineering: an inverse FORM approach for practice, Comput. Geotech. 111 (2019) 22–29.
[35] J. Ji, C. Zhang, Y. Gao, J. Kodikara, Effect of 2D spatial variability on slope reliability: a simplified FORM analysis, Geosci. Front. 9 (2018) 1631–1638.
[36] Y. Wang, P. Guo, H. Lin, X. Li, Y. Zhao, B. Yuan, et al., Numerical analysis of fiber-reinforced soils based on the equivalent additional stress concept, Int. J. Geomech. (2019), https://doi.org/10.1061/(ASCE)GM.1943-5622.00015044.
[37] C. Tang, W. Yang, Y. Fu, X.JE.G. Xu, A new approach to numerical method of modelling geological processes and rock engineering problems—continuum to discontinuum and linearity to nonlinearity, Eng. Geol. 49 (1998) 207–214.
[38] C. Tang, H. Liu, P. Lee, Y. Tsui, L. Tham, Numerical studies of the influence of microstructure on rock failure in uniaxial compression—part I: effect of heterogeneity, Int. J. Rock Mech. Min. Sci. 37 (2000) 555–569.
[39] H. Lin, X. Ding, R. Yong, W. Xu, S. Du, Effect of non-persistent joints distribution on shear behavior, C. R. Mecanique 347 (2019) 477–489, https://doi.org/10.1016/j.crme.2019.05.001.

[40] S. Pirmohammad, M. Hojjati Mengharpey, A new mixed mode I/II fracture test specimen: numerical and experimental studies, Theor. Appl. Fract. Mech. 97 (2018) 204–214, https://doi.org/10.1016/j.tafmec.2018.08.012.
[41] Y.X. Wang, S.B. Shan, C. Zhang, P.P. Guo, Seismic response of tunnel lining structure in a thick expansive soil stratum, Tunn. Undergr. Space Technol. 88 (2019) 250–259, https://doi.org/10.1016/j.tust.2019.03.0162.
[42] J. Justo, J. Castro, S. Cicero, M.A. Sánchez-Carro, R. Husillos, Notch effect on the fracture of several rocks: application of the theory of critical distances, Theor. Appl. Fract. Mech. 90 (2017) 251–258, https://doi.org/10.1016/j.tafmec.2017.05.025.
[43] H. Lin, W. Xiong, Z. Xiong, F. Gong, Three-dimensional effects in a flattened Brazilian disk test, Int. J. Rock Mech. Min. Sci. 74 (2015) 10–14, https://doi.org/10.1016/j.ijrmms.2014.11.006.
[44] J. Lemaitre, How to use damage mechanics, Nucl. Eng. Des. 80 (1984) 233–245.
[45] Y. Liu, F. Dai, A damage constitutive model for intermittent jointed rocks under cyclic uniaxial compression, Int. J. Rock Mech. Min. Sci. 103 (2018) 289–301, https://doi.org/10.1016/j.ijrmms.2018.01.046.
[46] X. Fan, H. Lin, H. Lai, R. Cao, J. Liu, Numerical analysis of the compressive and shear failure behavior of rock containing multi-intermittent joints, C. R. Mecanique 347 (2019) 33–48, https://doi.org/10.1016/j.crme.2018.11.001.
[47] R. Cao, W. Tang, H. Lin, X. Fan, Numerical analysis for the progressive failure of binary-medium interface under shearing, Adv. Civ. Eng. (2018) 4197172, https://doi.org/10.1155/2018/4197172.
[48] R.-h. Cao, P. Cao, H. Lin, G. Ma, Y. Chen, Failure characteristics of intermittent fissures under a compressive-shear test: experimental and numerical analyses, Theor. Appl. Fract. Mech. 96 (2018) 740–757, https://doi.org/10.1016/j.tafmec.2017.11.002.
[49] J. Mazars, G. Pijaudier-Cabot, Continuum damage theory—application to concrete, J. Eng. Mech. 115 (1989) 345–365.
[50] S. Gentier, J. Riss, G. Archambault, R. Flamand, D. Hopkins, Influence of fracture geometry on shear behavior, Int. J. Rock Mech. Min. Sci. 37 (2000) 161–174.
[51] Y. Li, J. Oh, R. Mitra, B. Hebblewhite, A constitutive model for a laboratory rock joint with multi-scale asperity degradation, Comput. Geotech. 72 (2016) 143–151.
[52] Z.C. Tang, C.C. Xia, S.G. Xiao, Constitutive model for joint shear stress–displacement and analysis of dilation, Chin. J. Rock Mech. Eng. 30 (2011) 917–925.
[53] S.Q. Yang, W.Y. Xu, C.D. Su, Study on statistical damage constitutive model of rock considering scale effect, Chin. J. Rock Mech. Eng. 24 (2005) 4484–4490.
[54] M. Huang, S.G. Du, Z.Y. Luo, X.H. Ni, Study of shear strength characteristics of simulation rock structural planes based on multi-size direct shear tests, Rock Soil Mech. 34 (2013) 3180–3186.
[55] B. Amadei, J. Wibowo, S. Sture, R.H. Price, Applicability of existing models to predict the behavior of replicas of natural fractures of welded tuff under different boundary conditions, Geotech. Geolog. Eng. 16 (1998) 79–128.
[56] O. Hungr, D.F. Coates, Deformability of joints and its relation to rock foundation settlement, Cangeotechj. 15 (1978) 239–249.
[57] M. Zhang, Y. Lu, Q. Yang, Failure probability and strength size effect of quasi-brittle materials, Chin. J. Rock Mech. Eng. 29 (2010) 1782–1789.
[58] H. Zhou, G.T. Cheng, Y. Zhu, J. Chen, J.J. Lu, G.J. Cui, et al., Experimental study of shear deformation characteristics of marble dentate joints, Rock Soil Mech. 40 (2019) 852–860.